

## 1

## Multiple Equilibria, Principles, and Derivations

### 1.1 General Considerations

Chemical reactions are initiated by accidental collision of molecules that have the potential (e.g., sufficient energy) to react with one another to be converted into products:



In living matter, it cannot be left to chance whether a reaction happens or not. At the precise time, the respective compounds must be selected and converted into products with high precision, while at unfavorable times spontaneous reactions must be prevented. An important prerequisite for this selectivity of reactions is the highly specific recognition of the required compound. Therefore, any physiological reaction occurring in the organism is preceded by a specific recognition or binding step between the respective molecule and a distinct receptor. The exploration of binding processes is substantial for understanding biological processes. The receptors can be enzymes as well as nonenzymatic proteins such as serum albumin, membrane transport systems, receptors for hormones or neurotransmitters, or nucleic acids. Generally, receptors are macromolecular in nature and thus considerably larger than the efficacious molecules, the *ligands*. For the binding process, however, both the macromolecule and its ligand must be treated as equivalent partners (unlike for enzyme kinetics, where the enzyme as catalyst does not take part in the reaction).

As a precondition for binding studies, specific binding must be established and unspecific association excluded. There exist various reasons for unspecific binding such as hydrophobic or electrostatic interactions (charged ligands can act as counterions for the surplus charges of proteins). A rough indicator for specific binding is the magnitude of the dissociation constant, which is mostly below  $10^{-3}$  M (although there are exceptions such as the binding of  $H_2O_2$  to catalase or glucose to glucose isomerase). Specific binding is characterized by a defined number of binding sites  $n$ , which is in stoichiometric relationship to the macromolecule. Ligands at high concentrations saturate the binding sites. Structurally similar compounds can displace the ligand from its binding site, while unrelated compounds have no effect. In contrast, unspecific binding has no defined number of binding sites, and the binding process is not saturable.

In the following sections, the processes leading to a specific interaction between a ligand and a macromolecule are described, that is, how the ligand finds its binding site and which factors determine the affinity. The essential mechanisms of interaction between ligand and macromolecule are then presented.

## 1.2 Diffusion

A prerequisite for any reaction of a ligand with a macromolecule is that the partners must find one another. A particle moves in the free space straight ahead with a kinetic energy of  $k_B T/2$ ,  $T$  being the absolute temperature and  $k_B$  the Boltzmann constant. According to Einstein's relationship, a particle with the mass  $m$  moving in a distinct direction with velocity  $v$  possesses kinetic energy  $mv^2/2$ . Combining both relationships, Eq. (1.1) follows:

$$v^2 = k_B T/m. \quad (1.1)$$

Accordingly, a macromolecule such as the enzyme lactate dehydrogenase ( $M_r = 140\,000$ ) would move at a rate of  $4\text{ m s}^{-1}$ , its substrate lactic acid ( $M_r = 90.1$ ) at  $170\text{ m s}^{-1}$ , a water molecule ( $M_r = 18$ ) at  $370\text{ m s}^{-1}$ . Enzyme and substrate will fly past one another like rifle bullets. In the dense fluid of the cell, however, the moving particles are permanently hampered and deflected from linear movement by countless obstacles: water molecules, ions, metabolites, macromolecules, and membranes. Thus, the molecule moves rather like a staggering drunkard than straight ahead. But this tumbling increases the collision frequency and the probability of distinct molecules meeting one another.

The distance  $x$  covered by a molecule in solution within time  $t$  in one direction depends on the diffusion coefficient  $D$  according to the equation:

$$x^2 = 2Dt. \quad (1.2)$$

The diffusion coefficient is itself a function of the concentration of the diffusing compound; in dilute solution, it can be considered as constant. It depends on the particle size, consistency of the fluid, and temperature. For small molecules in water, the coefficient is  $D = 10^{-5}\text{ cm}^2\text{ s}^{-1}$ . A cell with the length of  $1\text{ }\mu\text{m}$  is passed within  $500\text{ }\mu\text{s}$ ,  $1\text{ mm}$  within  $500\text{ s}$ , and so on; thus, for a thousandfold distance a millionfold time is required. This demonstrates that there exists no "diffusion velocity"; the movement of the molecules is not proportional to time but to its square root. A diffusing molecule does not remember its previous position; it does not strive systematically for new spaces but searches new regions randomly in undirected movement. As an example, a  $10\text{-cm-high}$  saccharose gradient ( $D_{\text{saccharose}} = 5 \times 10^{-6}\text{ cm}^2\text{ s}^{-1}$ ), used in ultracentrifugation for separation and molecular mass determination of macromolecules, has a life span of about 4 months. The tendency of the gradient to equalize its concentration is considerably low.

Equation (1.2) describes the one-dimensional diffusion of a molecule. For diffusion in a three-dimensional space over a distance  $r$ , the diffusion into the three

space directions  $x$ ,  $y$ , and  $z$  is assumed to be independent of each other:

$$r^2 = x^2 + y^2 + z^2 = 6Dt. \quad (1.3)$$

Mere meeting of ligand and macromolecule is not sufficient to accomplish specific binding; rather, the ligand must locate the binding site on the macromolecule. This is realized by translocation of the ligand volume  $4\pi R^3/3$  by the relevant distance of its own radius  $R$ . After a time  $t_x$ , the molecule has searched according to Eq. (1.3) for  $r = R$  a volume of

$$\frac{6Dt_x}{R^2} \cdot \frac{4\pi R^3}{3} = 8\pi DRt_x. \quad (1.4)$$

The volume searched per time unit is  $8\pi DR$ , and the probability of collision for a certain particle in solution is proportional to the diffusion coefficient and the particle radius.

At the start of a reaction  $A + B \rightarrow P$ , both participants are equally distributed in solution. Within a short time, molecules of one type, for example, B, become depleted in the vicinity of the molecule of the other type (A) not yet converted, so that a concentration gradient is formed. Consequently, a net flow  $\Phi$  of B molecules occurs in the direction of the A molecules located at a distance  $r$ ,

$$\Phi = \frac{dn}{dt} = DF \frac{dc}{dr}, \quad (1.5)$$

$n$  is the net surplus of molecules passing through an area  $F$  within time  $t$ , and  $c$  is the concentration of B molecules located at a distance  $r$  from the A molecules. This relationship in its general form is known as *Fick's first law of diffusion*. In our example of a reaction of two reactants,  $F$  has the dimension of a spherical surface with the radius  $r$ . Eq. (1.5) then changes into

$$\left( \frac{dc}{dr} \right)_r = \frac{\Phi}{4\pi r^2 D'} \quad (1.6)$$

$D'$  is the diffusion coefficient for the relative diffusion of the reactive molecules. Integration of Eq. (1.6) yields

$$c_r = c_\infty - \frac{\Phi}{4\pi r D'} \quad (1.7)$$

where  $c_r$  is the concentration of B molecules at the distance  $r$  and  $c_\infty$  the concentration at infinite distance from the A molecules. The last corresponds approximately to the average concentration of B molecules. The net flow  $\Phi$  is proportional to the reaction rate and that is again proportional to the average concentration  $c$  of those B molecules just in collision with the A molecules,  $r_{A+B}$  being the sum of the radii of an A and a B molecule:

$$\Phi = kc_{r_{A+B}} \quad (1.8)$$

where  $k$  is the rate constant of the reaction in the steady state, where  $c_r$  becomes equal to  $c_{r_{A+B}}$  and  $r$  equal to  $r_{A+B}$ . Substituted into Eq. (1.7), this becomes

$$c_{r_{A+B}} = \frac{c_\infty}{1 + \frac{k}{4\pi r_{A+B} D'}}. \quad (1.9)$$

The net flow under steady-state conditions is

$$\Phi = k_a c_\infty \quad (1.10)$$

where  $k_a$  is the relevant association rate constant. Equations (1.8)–(1.10) may thus be rewritten as

$$\frac{1}{k_a} = \frac{1}{4\pi r_{A+B} D'} + \frac{1}{k}. \quad (1.11)$$

This relation becomes linear in a graph plotting  $1/k_a$  against the viscosity  $\eta$  of the solution as, according to the *Einstein–Sutherland equation*, the diffusion coefficient at infinite dilution  $D_0$  is inversely proportional to the friction coefficient  $f$  and that again is directly proportional to the viscosity  $\eta$ :

$$D_0 = \frac{k_B T}{f} = \frac{k_B T}{6\pi\eta r}. \quad (1.12)$$

$1/k$  is the ordinate intercept. In the case of  $k \gg 4\pi r_{A+B} D'$ , the intercept is placed near the coordinate base; it becomes

$$k_a = 4\pi r_{A+B} D'. \quad (1.13)$$

This borderline relationship is known as the *Smoluchowski limit* for translating diffusion; the reaction is *diffusion controlled*. In contrast, in *reaction-controlled* reactions, the step following diffusion, that is, the substrate turnover, determines the rate. A depletion zone emerges around the enzyme molecule, as substrate molecules are not replaced fast enough. A *diffusion-limited dissociation* occurs if the dissociation of the product limits the reaction. Viewing two equally reactive spheres with radii  $r_A$  and  $r_B$  and diffusion coefficients  $D_A$  and  $D_B$ , we obtain for Eq. (1.13):

$$k_a = 4\pi r_{A+B} D' = 4\pi(r_A + r_B)(D_A + D_B). \quad (1.14)$$

By substituting Eq. (1.12) and with the approximation  $r_A = r_B$  and with  $D_0 = D_A = D_B$ , we obtain

$$k_a = \frac{8k_B T}{3\eta}. \quad (1.15)$$

Thus, the association rate constants for diffusion-controlled reactions are in the range  $10^9 - 10^{10} \text{ M}^{-1} \text{ s}^{-1}$ .

### 1.3 Modes of Ligand Binding

Uniform values should be obtained if the rate constants are exclusively determined by diffusion. In reality, however, the values of the rate constants of diffusion-controlled reactions of macromolecules vary within a range of more than five orders of magnitude. The reason for this variation is that, for successful binding of the ligand, random collision with the macromolecule is not sufficient. Both molecules must be in a favorable position to each other. This causes a considerable retardation of the binding process. On the other hand, attracting

forces could facilitate the interaction and direct the ligands toward their proper orientation. Under such conditions, rate constants can even surpass the values of mere diffusion control. Quantitative recording of such influences is difficult as they depend on the specific structures of both the macromolecule and the ligand. Theories have been developed to establish general rules for ligand binding.

Ligands approach a macromolecule at a rate according to Eq. (1.13), but only those meeting the correct site in the right orientation will react. If the binding site is considered as a circular area, forming an angle  $\alpha$  with the center of the macromolecule (Figure 1.1a), the association rate constant of Eq. (1.13) will be reduced by the sine of that angle:

$$k_a = 4\pi r_{A+B} D' \sin \alpha. \quad (1.16)$$

The necessity of appropriate orientation between ligand and binding site should be considered by the introduction of a suitable factor, depending on the nature of the reactive groups involved. It is also suggested that the ligand may associate unspecifically to the surface of the macromolecule, where it dissociates in a two-dimensional diffusion to find the binding site (*sliding model*; Berg, 1985, Figure 1.1b). The initial unspecific binding, however, cannot distinguish between the specific ligand and other metabolites, which may also bind and impede the two-dimensional diffusion. The *gating model* (Figure 1.1c) assumes the binding site to be opened and closed like a gate by changing the conformation of

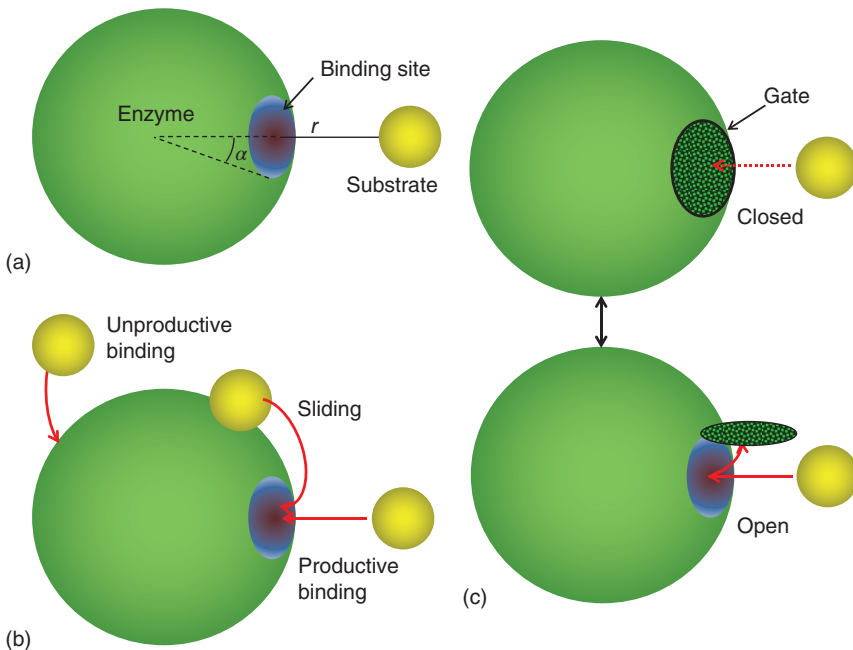


**Figure 1.1** Modes of ligand binding. (a) Interaction of a substrate molecule with its binding site on the enzyme. (b) Different types of interaction between ligand and macromolecule. (c) Gating.

the protein, thus modulating the accessibility for the ligand (McCammon and Northrup, 1981).

A basic limit for the association rate constant for the enzyme substrate is the quotient from the catalytic constant  $k_{\text{cat}}$  and the Michaelis constant  $K_m$  (cf. Section 2.2.1):

$$\frac{k_{\text{cat}}}{K_m} = \frac{k_{\text{cat}}k_1}{k_{-1} + k_2}. \quad (1.17)$$

For a diffusion-controlled reaction, the value is frequently around  $10^8 \text{ M}^{-1} \text{ s}^{-1}$ . The reaction rate for most enzyme reactions is determined more by the noncovalent steps during substrate binding and product dissociation rather than by the cleavage of bounds.

## 1.4 Interaction between Macromolecules and Ligands

### 1.4.1 Binding Constants

Binding of a ligand A to a macromolecule E



is described with the law of mass action, applying the association constant  $K_a$

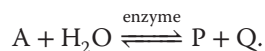
$$K_a = \frac{k_1}{k_{-1}} = \frac{[\text{EA}]}{[\text{A}][\text{E}]} \quad (1.19a)$$

or its reciprocal value, the dissociation constant  $K_d$

$$K_d = \frac{k_{-1}}{k_1} = \frac{[\text{A}][\text{E}]}{[\text{EA}]} \quad (1.19b)$$

Both notations are used: the association constant more frequently for the treatment of equilibria and the dissociation constant for enzyme kinetics. Here, the dissociation constant is employed throughout. The association constant has the dimension of a reciprocal concentration ( $\text{M}^{-1}$ ); the higher the numerical value, the higher the affinity. Conversely, dissociation constants possess the dimension of a concentration (M), and lower values indicate stronger binding. Equations (1.19a) and (1.19b) are not quite correct. The concentration terms should be transformed into activity terms by multiplying with an activity coefficient  $f$ , for example,  $a = f[\text{A}]$ . Since  $f$  approaches 1 in dilute solutions, this factor can be disregarded for enzyme reactions.

If one reaction component is present in such a large excess that its concentration change during the reaction can be neglected, its concentration can be combined with the rate constant. This applies especially for water, if it takes part in the reaction, especially in hydrolytic processes:



Water as a solvent with a concentration of  $55.56 \text{ mol l}^{-1}$  exceeds by far the nano- to millimolar amounts of all other components in an enzyme assay and

any change in its concentration will hardly be detectable. A binding constant for water cannot be determined, and the reaction is treated as if water is not involved:

$$K'_d = \frac{[A][H_2O]}{[P][Q]} = K_d[H_2O]; \quad K_d = \frac{[A]}{[P][Q]}.$$

Hydrogen ions, frequently involved in enzyme reactions, are treated in a similar manner. An apparent dissociation constant is defined:

$$K_{app} = K_d[H^+].$$

Contrary to genuine equilibrium constants, this constant is dependent on the pH value in the solution.

### 1.4.2 Binding to a Single Site

The binding constants for a distinct system can be determined applying the mass action law (Eq. (1.19)). For this, the concentrations of the free macromolecule [E], the free substrate [A], and the enzyme–substrate complex [EA] must be known, but this is usually not the case. Only the total amounts of macromolecule  $[E]_0$  and ligand  $[A]_0$  added to the reaction can be considered as known. They separate into free and bound components according to the mass conservation principle:

$$[E]_0 = [E] + [EA], \quad (1.20)$$

$$[A]_0 = [A] + [EA]. \quad (1.21)$$

As is described in Chapter 11, the portion of the ligand bound to the macromolecule  $[A]_{bound}$  can be obtained by binding experiments. If only one ligand molecule binds to the macromolecule as formulated in Eq. (1.18),  $[A]_{bound}$  is equal to [EA]. Substituting Eq. (1.20) into Eq. (1.19b) eliminates the free macromolecule concentration [E]:

$$[A]_{bound} = \frac{[E]_0[A]}{K_d + [A]}. \quad (1.22)$$

This equation describes the binding of a ligand to a macromolecule with one binding site, obviously the only possible mechanism for this case. Many enzymes and macromolecules, however, can bind more than one ligand molecule, and for such cases different binding mechanisms must be considered. They are presented in the following sections, where treatment and evaluation of the respective binding equations is also discussed.

## 1.5 Binding to Identical Independent Sites

### 1.5.1 General Binding Equation

Proteins and enzymes in living organisms are composed mostly of more than one subunit. Often all subunits are identical, and in such cases it can be taken that every subunit carries the same identical binding site for the ligand, so that the number  $n$  of binding sites is identical to the number of subunits. This is a plausible assumption, but it must be kept in mind that in the treatment of binding

processes identity means equality of binding constants. If the affinities of binding sites located on nonidentical subunits are the same by chance, or if a single subunit possesses more than one binding site with similar binding constants (e.g., due to gene duplication), this will not be differentiated by binding analysis and requires additional experiments.

For the binding of a ligand to a macromolecule with a single binding site only one binding mechanism exists, whereas several modes of binding are possible when the macromolecule carries more than one binding site, as shown in Figure 1.2. If the sites are identical, binding can either proceed independently (Figure 1.2b), or interactions between the sites can influence the binding course (Figure 1.2c). The same two possibilities exist if the sites are not identical (Figure 1.2d,e), but in both cases complex binding behavior is observed. These different binding modes are discussed in the following sections, while this section treats the simplest case, independent binding to identical sites. Actually, an independent binding process is already described by Eq. (1.22), since it should

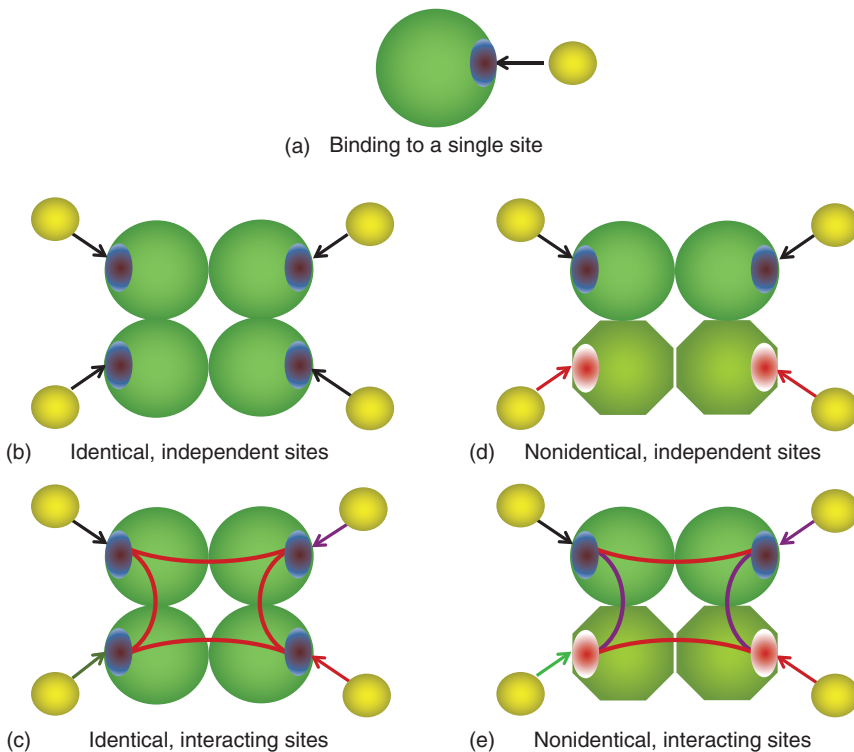


**Figure 1.2** Modes of binding of a ligand to a macromolecule. Binding to one single site (a) follows a normal binding course. If the macromolecule possesses more (e.g., four) binding sites, four different binding modes are possible. If the sites are identical and independent, normal binding occurs (b), whereas characteristic deviations appear if the binding sites interact with one another (c). Deviations also occur for the case of nonidentical binding sites even if they are independent (d) and the more if they interact with one another (e).



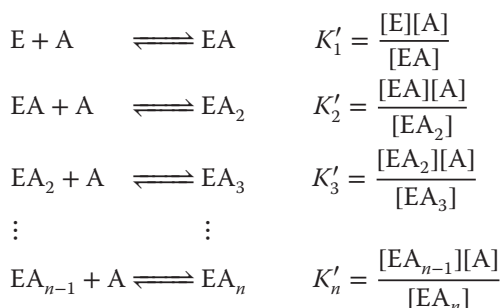
make no principal difference whether the binding occurs at a macromolecule with one single binding site or whether  $n$  independent sites are gathered on the same macromolecule. For this case, the macromolecule concentration  $[E]_0$  in Eq. (1.22) is replaced by  $[F]_0$ , the total amount of identical binding sites, which is related to the total macromolecule concentration by  $[F]_0 = n[E]_0$ :

$$[A]_{\text{bound}} = \frac{[F]_0[A]}{K_d + [A]} = \frac{n[E]_0[A]}{K_d + [A]} \quad (1.23a)$$

This equation differs from Eq. (1.22) in two respects. The numerator is extended by the number of binding sites, and  $[A]_{\text{bound}}$  can no longer be equated with  $[EA]$  but comprises all partially saturated forms of the macromolecule:

$$[A]_{\text{bound}} = [EA] + 2[EA_2] + 3[EA_3] + \cdots + n[EA_n] \quad (1.24)$$

The macromolecule is saturated stepwise:



Each step has its own dissociation constant. If, for independent binding, all individual dissociation constants are taken as equal, Eq. (1.23a) is obtained according to the upper derivation. It must be mentioned, however, that this is a simplified derivation, neglecting the fact that the ligand has various modes of orientation between the several binding sites of the macromolecule. In Box 1.1, the general binding equation is derived with regard to this case, but it can be seen, that albeit these complications finally Eq. (1.23a) results.

### Box 1.1 Derivation of the General Binding Equation

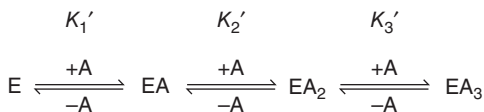
The dissociation constants of the individual binding steps are called *macroscopic* dissociation constants  $K'$  in contrast to *microscopic* (or *intrinsic*) binding constants  $K$  for binding to the individual sites of the macromolecule.

This is demonstrated in Scheme 1.1 for a macromolecule with three binding sites. The first binding step has one macroscopic dissociation constant  $K'_1$  but three microscopic dissociation constants, designated as  $K^1$ ,  $K^2$ , and  $K^3$ , according to the numbers of the binding sites  ${}_2E_3^1$ . Therefore, one ligand binding to the macromolecule can choose between three binding sites, and, consequently, three different macromolecule species can be formed. For the second binding step, three forms are also possible, but there are six ways to obtain these species;

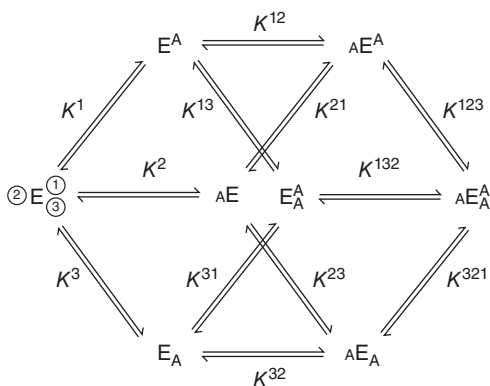
(Continued)

**Box 1.1 (Continued)**

Macroscopic binding constants



Microscopic binding constants



**Scheme 1.1** Macroscopic and microscopic binding constants of a macromolecule with three identical binding sites. The E-form at the left in the lower scheme shows the relative orientation and the denomination of the binding sites. The constants are designated according to the sequence of occupation, the last figure indicating the actual occupation.

accordingly, there exist six microscopic dissociation constants (e.g.,  $K^{12}$ ). From these three forms, three equilibria characterized by three microscopic binding constants (e.g.,  $K^{123}$ ) lead to the one fully saturated macromolecule form. The complete binding process is described by 3 macroscopic and 12 microscopic dissociation constants (Scheme 1.1). The relationship between both types of constants can be established by applying the respective mass action laws. The macroscopic dissociation constant of the first binding step is defined as

$$K_1' = \frac{[E][A]}{[EA]} = \frac{[E][A]}{[E^A] + [{}_A E] + [E_A]}$$

The microscopic binding constants are used to replace the individual macromolecule forms

$$\begin{aligned} K^1 &= \frac{[E][A]}{[E^A]}; & [E^A] &= \frac{[E][A]}{K^1} \\ K^2 &= \frac{[E][A]}{[{}_A E]}; & [{}_A E] &= \frac{[E][A]}{K^2} \\ K^3 &= \frac{[E][A]}{[E_A]}; & [E_A] &= \frac{[E][A]}{K^3} \end{aligned}$$

$$K'_1 = \frac{1}{\frac{1}{K^1} + \frac{1}{K^2} + \frac{1}{K^3}}.$$

If the three binding sites are identical, the microscopic constants can be equalized,  $K^1 = K^2 = K^3 = K$ , and both types of constants are related by  $K' = K/3$ .

Correspondingly, the second binding step is

$$K'_2 = \frac{[EA][A]}{[EA_2]} = \frac{([E^A] + [{}_A E] + [E_A])[A]}{[{}_A E^A] + [E^A] + [{}_A E_A]}$$

$$K^{12} = \frac{[E^A][A]}{[{}_A E^A]}; \quad [{}_A E^A] = \frac{[E^A][A]}{K^{12}}, \quad \text{etc., hence}$$

$$K'_2 = \frac{K^{13}K^{21}K^{23} + K^{12}K^{13}K^{23} + K^{13}K^{21}K^{32}}{K^{13}K^{23} + K^{12}K^{23} + K^{13}K^{21}}.$$

For  $K^{12} = K^{13} = \dots = K$ ,  $K'_2 = K$ .

The third binding step is

$$K'_3 = \frac{[EA_2][A]}{[EA_3]} = \frac{([{}_A E^A] + [E^A] + [{}_A E_A])[A]}{[{}_A E^A]},$$

$$K^{123} = \frac{[{}_A E^A][A]}{[{}_A E^A]}; \quad [A E^A] = \frac{K^{123}[{}_A E^A]}{[A]}, \quad \text{etc.}$$

For  $K^{123} = K^{132} = \dots = K$ ,  $K'_3 = 3K$ .

Even if all microscopic dissociation constants are identical, they differ from the macroscopic ones, and there are differences between each binding step. The general relationship between both types of dissociation constants for  $n$  binding sites is

$$K'_d = K_d \frac{i}{n - i + 1}, \quad (1)$$

where  $i$  represents the respective binding step. Ligands occupying stepwise a macromolecule with identical sites have  $\Omega$  possibilities of orientation, depending on the respective binding step  $i$ :

$$\Omega = \frac{n!}{(n - i)!i!} \quad (2)$$

For the derivation of the general binding equation, a saturation function  $r$  is defined as the quotient from the portion of bound ligand to the total amount of the macromolecule:

$$r = \frac{[A]_{\text{bound}}}{[E]_0} = \frac{[EA] + 2[EA_2] + 3[EA_3] + \dots + n[EA_n]}{[E] + [EA] + [EA_2] + [EA_3] + \dots + [EA_n]}. \quad (3)$$

The concentrations of the individual macromolecule forms are not accessible experimentally and are replaced by the macroscopic dissociation constants:

$$K'_1 = \frac{[E][A]}{[EA]}; \quad [EA] = \frac{[E][A]}{K'_1}$$

$$K'_2 \frac{[EA][A]}{[EA_2]}; \quad [EA_2] = \frac{[EA][A]}{K'_2} = \frac{[E][A]^2}{K'_1 K'_2}$$

(Continued)



Equation (1.23a) can reduce to the following equation, already obtained by the simplified derivation:

$$r = \frac{[A]_{\text{bound}}}{[E]_0} = \frac{n[A]}{K_d + [A]} \quad (6)$$

The authorship of the binding equation is ascribed to Irvin Langmuir, who developed such a relationship in 1916 for the adsorption of gases to solid surfaces, although Adrian J. Brown and Victor Henri derived a similar equation in 1900, which was revised by Leonor Michaelis and Maud Menten in 1913. This *Michaelis–Menten equation* is of fundamental importance for enzyme kinetics (see Section 3.2.1).

Equation (1.23a) (respectively, Eq. (6) in Box 1.1) describes the relationship between the free and the bound ligand. By successive increase of the free ligand a saturation curve is obtained (Figure 1.3a), which follows mathematically the function of a right-angle hyperbola (the correlation between the saturation curve and a hyperbola is explained in Section 3.3.1.1, Box 3.1). At extremely high concentrations of the ligand, ( $[A] \rightarrow \infty$ )  $K_d$  in the denominator of Eq. (1.23a) can be ignored, and the curve approaches  $n[E]_0$  (respectively  $n$  for Eq. (6) Box 1.1), from which the number of binding sites can be obtained. Half of this value,  $n[E]_0/2$  respectively  $n/2$ , that is, half saturation, indicates the position where the free ligand concentration equals the value of the dissociation constant,  $[A] = K_d$ , a possibility to determine this value. Thus, both the dissociation constant and the number of binding sites can be obtained from the saturation curve (Figure 1.3a).

There exist three principally equivalent modes for plotting binding data. The amount of bound ligand  $[A]_{\text{bound}}$  obtained from the experiment can be plotted directly against the free ligand concentration  $[A]$ . Saturation will be reached at  $n[E]_0$ . It is more convenient to take the saturation function  $r$  dividing  $[A]_{\text{bound}}$  by  $[E]_0$ , as discussed already. If  $r$  is further divided by  $n$ , the function  $\bar{Y}$  is obtained:

$$\bar{Y} = \frac{[A]_{\text{bound}}}{n[E]_0} = \frac{[A]}{K_d + [A]} \quad (1.23b)$$

In this case, the value of the saturation becomes 1. The function  $\bar{Y}$  is used if different mechanisms are compared theoretically (without defining  $n$ ) or, experimentally, when the portion of bound ligand is not directly known, as in spectroscopic titrations (see Section 1.5.2.2).

## 1.5.2 Graphic Representations of the Binding Equation

### 1.5.2.1 Direct and Linear Diagrams

Generally binding studies should yield three kinds of information:

- The affinity of the macromolecule for the ligand, represented by the value of the dissociation constant  $K_d$
- The number of binding sites  $n$
- The respective binding mechanism.

The goal of graphic representations is to obtain this information in a clear, unambiguous manner. There exist different kinds of graphic representations, and it must be decided which will be the most appropriate for the respective experimental data. Usually, the data will be represented in different plots because special aspects will become more obvious in one type than in another, although, as a rule, missing information cannot be recalled by any representation.

The direct plotting of the data of a binding experiment has already been shown in Figure 1.3a. This mode of plotting is recommended as a primary step, since the data suffer no distortion, especially with respect to the error distribution. A difficulty is the estimation of saturation. Because saturation can be reached only at infinity, the value of full saturation is frequently underestimated. It must be kept in mind that the experiment yields no continuous curve rather a scattering set of single data points. This uncertainty also influences the accuracy of the determination of  $n$  and  $K_d$ . Nonlinear regression should be applied to improve the analysis.

Instead of direct plotting,  $r$  can be plotted against  $\log [A]$  in a *semilogarithmic diagram* as well. This procedure is recommended especially when larger concentration ranges have to be covered, which cannot be resolved completely in the direct plot. In the semilogarithmic diagram, the saturation curves have a sigmoidal shape, and the logarithm of  $K_d$  is obtained from half saturation (Figure 1.3b).

Besides the problems of determination of the constants, it is also not easy with nonlinear plots to recognize deviations from the normal saturation course and to detect possible alternative binding mechanisms. Weak deviations will easily be

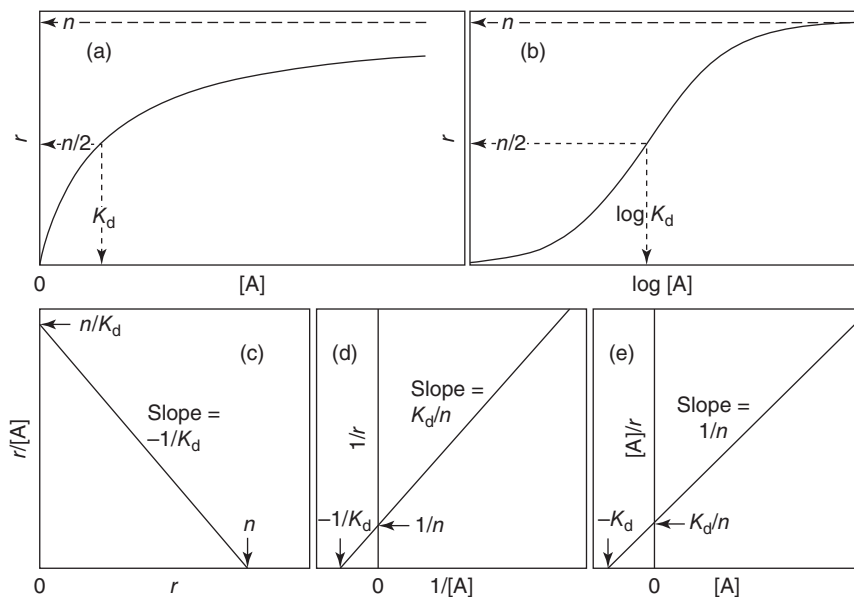


**Figure 1.3** Modes of representing binding data. (a) Direct plot; (b) semilogarithmic plot; (c) Scatchard plot; (d) double-reciprocal plot; and (e) Hanes plot.

hidden behind the data scatter. With linear diagrams, it can be discerned clearly whether a special mechanism fits a straight line or not; on the other hand, these diagrams exhibit other disadvantages.

Three simple linear transformations of the binding equation exist. The *double-reciprocal plot*, ascribed to Klotz (1946) (although he was not the original author; the problem of proper denomination of special diagrams is discussed in Section 3.3.1.3) is based on the reverse form of Eq. (1.23a):

$$\frac{1}{r} = \frac{1}{n} + \frac{K_d}{n[A]}. \quad (1.25)$$

Plotting  $1/r$  against  $1/[A]$  should yield a straight line, intercepting the ordinate at  $1/n$  and the abscissa at  $-1/K_d$ . Therefore, both constants can easily be obtained by extrapolation (Figure 1.3d). Alternative mechanisms show characteristic deviations from linearity. The double-reciprocal plot has the advantage of separation of the variables (in contrast to the other two linear diagrams); however, due to the reciprocal entry, strong distortions of the error limits are observed, which are compressed to the high ligand range and expanded to the low ligand range. Linear regression is not applicable and especially the determination of  $n$  at the ordinate intercept often becomes dubious with scattering data.

For the analysis of binding data, the diagram of Scatchard (1949) is preferred. It allows an unequivocal determination of the value of  $n$ , which is of great importance for many analysis. Multiplication of Eq. (1.25) by  $rn/K_d$  yields

$$\frac{r}{[A]} = \frac{n}{K_d} - \frac{r}{K_d}. \quad (1.26)$$

Plotting  $r/[A]$  versus  $r$  yields a straight line intersecting the abscissa at  $n$  and the ordinate at  $n/K_d$  (Figure 1.3c). In this diagram, the error limits increase toward high ligand concentrations, but the effect is lower than with the double-reciprocal diagram and linear regression is often applied. Although the variables are not separated, this is the most reliable linear diagram.

A third diagram is obtained by multiplying Eq. (1.25) by  $[A]$ :

$$\frac{[A]}{r} = \frac{[A]}{n} + \frac{K_d}{n}. \quad (1.27)$$

This diagram is equivalent to the *Hanes plot* in enzyme kinetics, but for the analysis of binding data it is seldom used. By plotting  $[A]/r$  versus  $[A]$ ,  $K_d/n$  follows from the ordinate and  $-K_d$  from the abscissa intercept (Figure 1.3e). An advantage of this representation is the nearly constant error limit.

### 1.5.2.2 Analysis of Binding Data from Spectroscopic Titrations

Although methods for the determination of binding are described later (cf. Chapter 13), theoretical aspects of the analysis are discussed here. Spectroscopic titrations are convenient methods to study binding processes, but the data need a special treatment as the diagrams discussed so far cannot be applied directly. The main difference from other binding methods is that the share of the free ligand  $[A]$  cannot be obtained directly by experiment and also the share of bound ligand is observed only as a relative spectral change and not as a molar concentration. In the experimental procedure, usually increasing amounts of the ligand are

successively added to a constant amount of the macromolecule in a photometric cuvette. The spectral change induced by binding of the ligand is recorded. For the evaluation of the data, only the total amount of the added ligand  $[A]_0$  is known, while for the conventional plots (Figure 1.3) the free ligand concentration  $[A]$  is required. In similar diagrams used in enzyme kinetics, usually the total substrate concentration is taken, since due to the very low (*catalytic*) enzyme concentrations the share of bound substrate can be ignored and the amounts of total and free ligand can be equated. In binding measurements, however, the macromolecule is present in high concentrations to get a detectable signal. Therefore, the share of bound ligand cannot be ignored and  $[A]$  cannot be displaced by  $[A]_0$ . The direct plotting of the extent of the spectral change against  $[A]_0$ , as obtained from the experiment, yields a *titration curve*. For evaluation, it must be either treated in a special manner or converted into conventional plots as shown in Figure 1.3. This is discussed in the following paragraphs. Another representation, the Dixon plot, is discussed in Section 3.3.1.1.

In the low concentration range of the titration curve, as long as the condition  $[A]_0 < [E]_0$  holds, nearly all the added ligands bind to the macromolecule and no free ligand appears; thus  $[A]_0 \sim [A]_{\text{bound}}$ . Under these conditions, the added ligand is directly related to the spectral change, and the initial part of the titration curve follows a straight line through which a tangent can be drawn. This tangent represents, also in its extension, the share of the bound ligand, while at higher concentrations the curve deviates from the tangent because of the appearance of free ligand when the macromolecule becomes successively saturated (Figure 1.4a). The spectral signal increases upon further addition of ligand as long as free binding sites are available, but the increase ceases until all sites are occupied. The curve reaches a saturation plateau through which an asymptotic line can be drawn. The extent of the optical signal at the position of the asymptotic line corresponds to the amount of ligand bound to all available binding sites:  $n[E]_0$ . This value can be obtained directly from the abscissa coordinate of the position, where the initial tangent meets the saturation asymptote (see Figure 1.4a). Initially, the extent of the optical signal is taken as ordinate scale. After the experiment, these relative values must be converted into  $\bar{Y}$  values, setting the saturation equal to  $\bar{Y} = 1$ . The total amount

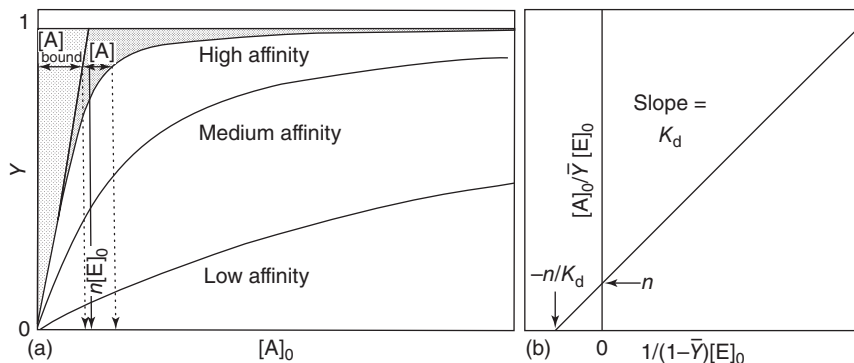


Figure 1.4 Evaluation of spectroscopic titrations. (a) Direct plotting and (b) Stockell plot.



of ligand  $[A]_0$  indicated at the abscissa is the sum of free and bound ligands. Both shares can be separated drawing vertical lines from any point of the curve to the ordinate. These lines are divided by the origin tangent into two sections, the right one indicating the share of the free and the left one the bound ligand. With the exception of the points fitting the initial tangent, all data points of the curve can be converted in this manner and with this information the conventional diagrams described in Section 1.5.2.1 can be drawn and evaluated accordingly.

A severe disadvantage of this procedure is the fact that it depends essentially on the alignment of tangents. With strongly scattering values or if the assumption does not hold that at low concentrations all added ligand binds, the alignment will become incorrect. This must be considered especially in the case of low-affinity binding, where there is a tendency to align the tangent too flat. Since both asymptotic lines represent the case of infinite high affinity, the more reliable the evaluation of the titration curve, the higher the actual affinity.

To circumvent the uncertainty of the initial tangent, the titration curve can be directly linearized according to a procedure suggested by Stockell (1959), where the free ligand concentration in Eq. (1.23a) is replaced by  $[A]_0$ . The spectral signal is converted into values for  $\bar{Y}$ , saturation being defined as  $\bar{Y} = 1$ . To derive a linear relationship,  $r = n\bar{Y} = n[EA]/[E]_0$  is substituted into Eq. (1.25), and  $[A]_{\text{bound}} = n[EA]$ :

$$\frac{1}{\bar{Y}} = 1 + \frac{K_d}{[A]_0 - n[EA]} = 1 + \frac{K_d}{[A]_0 - n\bar{Y}[E]_0}.$$

Transformation to

$$\frac{[A]_0}{\bar{Y}} - [A]_0 = n[E]_0(1 - \bar{Y}) + K_d$$

results in

$$\frac{[A]_0}{[E]_0\bar{Y}} = \frac{K_d}{[E]_0(1 - \bar{Y})} + n. \quad (1.28)$$

In this diagram (Figure 1.4b), a straight line should result, and  $n$  and  $K_d$  can be obtained from the ordinate and abscissa intercepts, respectively. There still remains the uncertainty of the saturation asymptote, which is required for the definition of  $\bar{Y} = 1$ . Therefore, the measurements must be extended far into the saturation range. This plot is very sensitive even for weak deviations from the theoretical function, and a wrong saturation value may distort the whole curve. For this reason, alternative mechanisms or artificial influences are difficult to discern in the Stockell plot.

A different presentation of binding data was suggested by Job (1928). The total concentrations of the ligand and macromolecule are kept constant and only the molar proportions of both components are varied.  $X$  is the mole fraction of the macromolecule and  $Y$  is that of the ligand,  $X + Y = 1$ . This expression is plotted against the measured values  $M$  of an optical signal or the enzyme activity, which must be proportional to  $[A]_{\text{bound}}$ . A maximum curve is obtained, as shown in Figure 1.5. The position of the maximum corresponds to the stoichiometry of both binding partners. Tangents can be aligned from  $X = 0$  and  $Y = 0$ , and their

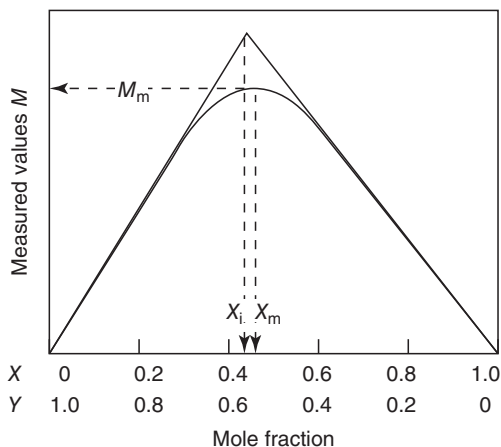


Figure 1.5 Job plot for the evaluation of binding data.

intercept marks the position of the maximum. The maximum is at  $X = Y = 0.5$  for a 1 : 1 stoichiometry, at  $X = 0.33, Y = 0.66$  for a 1 : 2, and at  $X = 0.25, Y = 0.75$  for a 1 : 4 stoichiometry, corresponding to ligand–macromolecule complexes  $EA$ ,  $EA_2$ , and  $EA_4$ , respectively. However, the position of the maximum indicates only the relative ratio; it will be, for example, at the same position for a 1 : 1 ( $EA$ ), a 2 : 2 ( $E_2A_2$ ), or a 4 : 4 ( $E_4A_4$ ) stoichiometry.

$K_d$  can be obtained from the ratio of the actual measured value at the maximum,  $M_m$ , to the saturation value,  $M_\infty$ , according to Eq. (1.30).

Their common intercept has the value

$$\frac{Y_i}{X_i} = \frac{K_d + nc_0}{K_d + c_0}. \quad (1.29)$$

$X_i$  and  $Y_i$  are the mole fractions of macromolecule and ligand at the intercept,  $c_0 = [E]_0 + [A]_0$  is the (constant) sum of the total concentrations of macromolecule and ligand. If  $c_0 \gg K_d$ , then  $X_i/Y_i = n$ . Here, the stoichiometry of the binding can be taken from the ratios of the mole fractions at the tangent intercept. If  $c_0 \ll K_d$ , then  $X_i/Y_i = 1$ ; the curve takes a symmetrical shape and the intercept always has the value 1, irrespective of the actual number of binding sites. This is a disadvantage of the Job plot. It can be circumvented as long as the sum of the macromolecule and ligand concentrations is higher than the value of the dissociation constant. If  $n$  is known,  $K_d$  can be calculated from Eq. (1.29), whereby the condition  $c_0 \sim K_d$  should be considered.  $K_d$  can also be obtained from the maximum of the curve in Figure 1.5 according to

$$K_d = \frac{(\alpha n + \alpha - n)^2 c_0}{4\alpha n}. \quad (1.30)$$

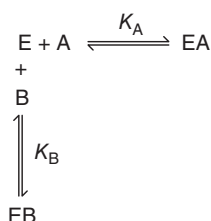
Here,  $\alpha$  represents the ratio of the actual measured value at the maximum,  $M_m$ , to the saturation value,  $M_\infty$ .

### 1.5.3 Binding of Different Ligands, Competition

Due to the high binding specificity of proteins and especially of enzymes, usually only the physiological ligand or the enzyme substrate will be able to bind,

while all other metabolites will be excluded. However, this selection cannot be absolute, and compounds with high structural homology to the ligand may also be accepted. Knowing the configuration of the binding site or the active center, such analogs can be designed and may bind with similar or sometimes even with higher affinity than the natural ligand. In some cases, they imitate the function of the ligand, but mostly they are inactive and block the binding site for the native ligand, preventing its action and revealing an antagonistic effect. This *competition* for a distinct binding site of two or more compounds is a valuable tool to investigate specific binding; thus, the action of drugs depends frequently on the antagonistic effect (e.g.,  $\beta$ -receptor blocker). Competition is also a valuable tool in cases where binding of the ligand is difficult to detect, for example, because of the lack of a measurable signal. In such cases, a fraction of the ligand is converted into a detectable form, for example, by fluorescent labeling. At first, the binding characteristic and the dissociation constant of the labeled ligand (B) are determined, and thereafter the measurements are repeated in the presence of constant amounts of the unlabeled ligand A. In the following, the derivation of the dissociation constant for this ligand is described.

The competition can be described by the following scheme:



The binding affinities are expressed by the dissociation constants  $K_A$  and  $K_B$  for both compounds:

$$K_A = \frac{[E][A]}{[EA]} \quad \text{and} \quad K_B = \frac{[E][B]}{[EB]} \quad (1.31a)$$

The total amount of the macromolecule is

$$[E]_0 = [E] + [EA] + [EB].$$

$[E]$  and  $[EB]$  are replaced by  $K_A$  and  $K_B$  in Eq. (1.31a):

$$[E]_0 = \frac{K_A[EA]}{[A]} \left( 1 + \frac{[B]}{K_B} \right) + [EA].$$

By conversion, the following expression for  $[EA]$  is obtained:

$$[EA] = \frac{[E]_0[A]}{[A] + K_A \left( 1 + \frac{[B]}{K_B} \right)}.$$

For a macromolecule with  $n$  binding sites,

$$r = \frac{n[A]}{[A] + K_A \left( 1 + \frac{[B]}{K_B} \right)}. \quad (1.32)$$

The double-reciprocal relationship is

$$\frac{1}{r} = \frac{1}{n} + \frac{K_A}{n[A]} \left( 1 + \frac{[B]}{K_B} \right) \quad (1.33)$$

and the Scatchard equation is

$$\frac{r}{[A]} = \frac{n}{K_A \left( 1 + \frac{[B]}{K_B} \right)} - \frac{r}{K_A \left( 1 + \frac{[B]}{K_B} \right)}. \quad (1.34)$$

Compared with the general binding equation, there are now two variable concentration terms, but as long as one of them (e.g., B) remains constant and only A is altered, the term within the brackets will remain constant and the behavior corresponds to the general binding equation with a hyperbolic curve (Figure 1.6a) with the only difference that the value of  $K_A$  is increased by the value of the term in brackets. If, in a second test series, another (constant) concentration of B is taken, again a hyperbolic curve with an altered  $K_A$  is obtained. In this manner, a series of hyperbolic curves are obtained. All can be linearized in the double-reciprocal plot (Figure 1.6b), the Scatchard plot (Figure 1.6c), and the Hanes plot (Figure 1.6d). Remarkable patterns of the lines with a common ordinate intercept in the double-reciprocal diagram, a joint abscissa intercept in the Scatchard plot, and parallel lines in the Hanes plot are obtained. These patterns can be taken as indicative of a competitive mechanism.

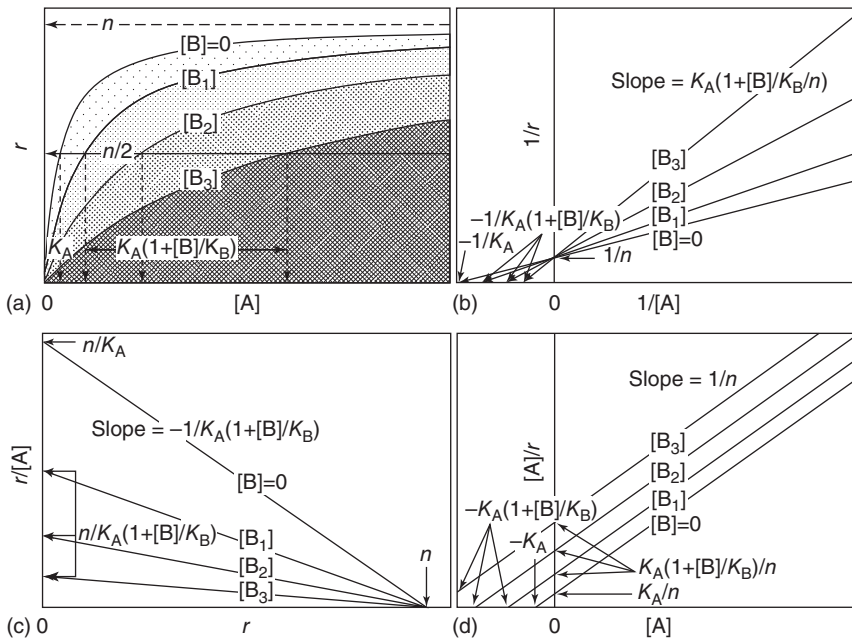
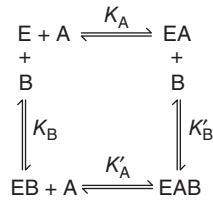


**Figure 1.6** Competition of two ligands for the same binding site. The concentration of ligand A is altered in the presence of constant amounts of ligand B, which vary from curve to curve. (a) Direct plot, (b) double-reciprocal plot, (c) Scatchard plot, and (d) Hanes plot.

In the double-reciprocal diagram, the dissociation constant for ligand A,  $K_A$ , can be obtained in the absence of B directly from the abscissa intercept, and with the knowledge of this constant the dissociation constant for B,  $K_B$ , can be derived also from the abscissa intercept in the presence of B (Figure 1.6b). From the other linear plots, the constants can be derived in as shown in Figure 1.6c,d. Further procedures for the analysis of competition in enzyme kinetic studies are described in Section 4.2.2.2. But in contrast to enzyme kinetics in binding studies, competitive and noncompetitive mechanisms are not discernible by graphical analysis, as shown in the following section.

#### 1.5.4 Noncompetitive Binding

Also in this case, two different ligands, A and B, bind to the same macromolecule but at different sites. They do not displace one another, but the ligand bound first influences the binding of the second one, for example, by steric or electrostatic interactions, which are mostly repulsive but can also be attractive. Consequently, each ligand possesses two dissociation constants, one,  $K_A$ , respectively,  $K_B$ , for binding to the free macromolecule, and the second one,  $K'_A$ ,  $K'_B$ , for binding to the EA or EB complex:



$K'_A$  and  $K'_B$  are defined as

$$K'_A = \frac{[EB][A]}{[EAB]} \quad \text{and} \quad K'_B = \frac{[EA][B]}{[EAB]}, \quad (1.31b)$$

considering Eq. (1.31a) all four constants are linked.

$$\frac{K_A}{K_B} = \frac{K'_A}{K'_B}. \quad (1.35)$$

The total amount of the macromolecule is

$$[E]_0 = [E] + [EA] + [EB] + [EAB]$$

The individual macromolecule forms can be substituted by the dissociation constants applying Eqs (1.31a, b):

$$\begin{aligned}
 [E]_0 &= [E] + \frac{[E][A]}{K_A} + \frac{[E][B]}{K_B} + \frac{[E][A][B]}{K_A K'_B}, \\
 [E] &= \frac{[E]_0}{1 + \frac{[A]}{K_A} + \frac{[B]}{K_B} + \frac{[A][B]}{K_A K'_B}}.
 \end{aligned}$$

The fraction of  $[A]_{\text{bound}}$  is

$$[A]_{\text{bound}} = [EA] + [EAB] = \frac{[E][A]}{K_A} + \frac{[E][A][B]}{K_A K'_B},$$

$$[A]_{\text{bound}} = \frac{\frac{[E]_0[A]}{K_A} \left(1 + \frac{[B]}{K'_B}\right)}{1 + \frac{[A]}{K_A} + \frac{[B]}{K_B} + \frac{[A][B]}{K_A K'_B}}.$$

The final equation for the noncompetitive binding is obtained by replacing  $[A]_{\text{bound}}$  by  $r = [A]_{\text{bound}}/[E]_0$ , assuming  $n$  binding sites and multiplying by  $K_A$ :

$$r = \frac{n[A] \left(1 + \frac{[B]}{K'_B}\right)}{K_A \left(1 + \frac{[B]}{K_B}\right) + [A] \left(1 + \frac{[B]}{K'_B}\right)}. \quad (1.36)$$

Obviously, Eq. (1.36) can be reduced to the normal binding equation if  $K_B = K'_B$  and, consequently,  $K_A = K'_A$ , that is, if both ligands do not interact with one another. Transformation into the double-reciprocal form yields

$$\frac{1}{r} = \frac{1}{n} + \frac{K_A \left(1 + \frac{[B]}{K_B}\right)}{n[A] \left(1 + \frac{[B]}{K'_B}\right)}. \quad (1.37)$$

This gives a pattern of straight lines with a joint ordinate intercept similar to that shown in Figure 1.6b for competitive inhibition. Accordingly, the Scatchard plot

$$\frac{r}{[A]} = n \frac{\left(1 + \frac{[B]}{K'_B}\right)}{K_A \left(1 + \frac{[B]}{K_B}\right)} - r \frac{\left(1 + \frac{[B]}{K'_B}\right)}{K_A \left(1 + \frac{[B]}{K_B}\right)} \quad (1.38)$$

yields a pattern of straight lines, as shown in Figure 1.6c (the analogous situation holds for the Hanes plot, Figure 1.6d). Surprisingly, both competitive and noncompetitive binding are indistinguishable by graphic analysis. This is a serious source of misinterpretation, the more so, as both corresponding mechanisms in enzyme kinetics are readily distinguishable by graphic analysis (see Section 4.2.1.2). The reason for this discrepancy is not quite obvious. In enzyme kinetics, a similar situation exists with respect to the partially competitive inhibition, which yields just the same pattern in linearized diagrams as the competitive mechanism (Section 4.2.3.3). In fact, noncompetitive binding is analogous to partially competitive inhibition and not to noncompetitive inhibition. In noncompetitive inhibition, only the enzyme–substrate complex  $[EA]$  is enzymatically active, while the complex with both substrate and inhibitor  $[EAI]$  is inactive. In contrast, in partially competitive inhibition both complexes are equally active. This is just the situation in binding studies, where the amount of

$[A]_{\text{bound}}$  is obtained experimentally as the sum of  $[EA]$  and  $[EAB]$ , considering both as equally active. It can be differentiated between both mechanisms and misinterpretations avoided by a simple control. Plotting the slopes of the straight lines of the double-reciprocal diagrams against the concentration of the second ligand B must yield a straight line (with  $-K_B$  as abscissa intercept) for competitive binding, while the curve deviates from linearity in the case of noncompetitive binding. Such *secondary plots* can also be derived from the Scatchard and the Hanes diagram and are discussed in more detail in Section 4.2.1.1.

## 1.6 Binding to Nonidentical, Independent Sites

Various enzymes, membrane receptors, and other macromolecules carry different binding sites for the same ligand. They may be found at the same subunit or polypeptide chain, but more frequently they are located at separate nonidentical subunits. The bacterial tryptophan synthase, for example, consists of two types of subunits ( $\alpha, \beta$ ), each binding indole as the intermediate of the enzyme reaction. The enzyme molecule consists of two copies of each type of subunit, corresponding to a structure  $\alpha_2\beta_2$ , so that binding to identical and nonidentical sites occurs simultaneously. Identical sites are called *binding classes*, one macromolecule can possess several ( $m$ ) binding classes, each with several identical binding sites ( $n_1, n_2, n_3, \dots$ ).

Obviously, a ligand binding to such a macromolecule occupies the site with the highest affinity first. Occupation of the lower affinity sites requires higher ligand concentrations. Assuming independent binding, each binding class is saturated according to the general binding equation Eq. (1.23a). Correspondingly, the total binding process is the sum of the individual saturation functions for each binding class:

$$r = \frac{n_1[A]}{K_{d1} + [A]} + \frac{n_2[A]}{K_{d2} + [A]} + \dots + \frac{n_m[A]}{K_{dm} + [A]}. \quad (1.39)$$

$K_{d1}, K_{d2}$ , and so on, are the dissociation constants of the individual binding classes. Each binding process follows a normal hyperbolic binding curve. The resulting function is a superposition of the different hyperbolae (Figure 1.7a). It shows a steep increase in the low concentration range of the ligand, where the high-affinity site becomes occupied. At higher ligand concentrations, most high-affinity sites are saturated and occupation of the low-affinity sites starts. The rise of the saturation curve is now clearly smoother. Because of the superposition of different saturation functions, the resulting curve does not possess a pure hyperbolic shape, but the deviation is not easy to recognize, especially with scattering data points. For analysis, linearized plots are helpful, because they show characteristic deviations from linearity. This is demonstrated in Figure 1.7b–d, where the individual linear curves for a high- and a low-affinity site and the resulting composed function are drawn in the nonlinear and different linear representations.

It is much easier to create a composed function from the partial functions than to resolve the individual functions for the separate binding sites from a composed

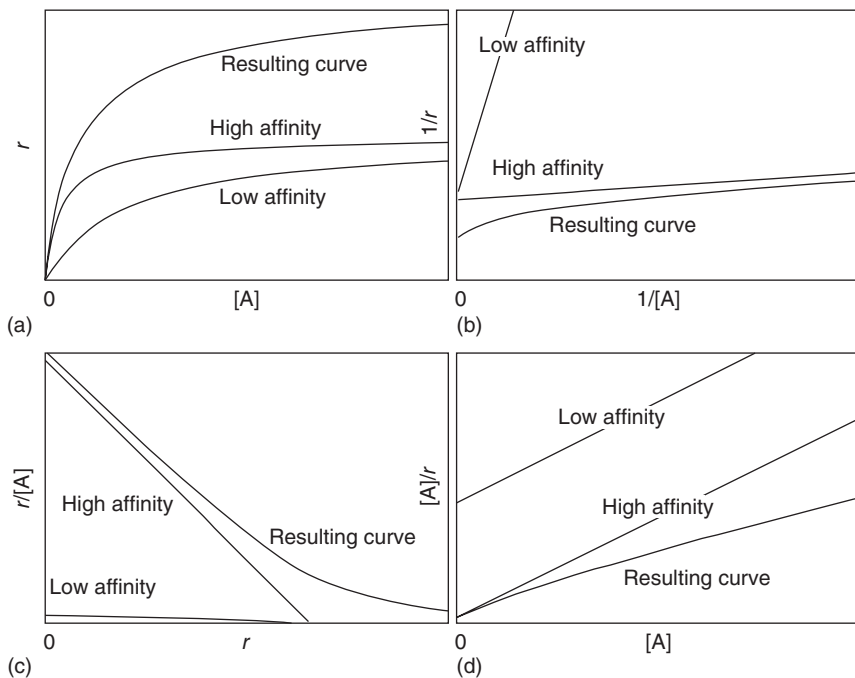


**Figure 1.7** Binding of a ligand to two binding classes of different affinities. The individual straight lines for the high- and the low-affinity sites and the resulting curves are shown. (a) Direct plotting, (b) double-reciprocal plot, (c) Scatchard plot, and (d) Hanes plot.

function obtained by experimental results. There are several unknown values to be determined, such as the number of binding classes involved, the number of identical sites per binding class, and the values of the dissociation constants. All these parameters cannot be obtained from one curve. As can be seen from Figure 1.7, the individual functions are not merely the asymptotes to the extreme ranges of the resulting curve, although it may be assumed that at very low and very high ligand concentrations the high- and low-affinity sites, respectively, are occupied preferentially. Rosenthal (1967) suggested a graphical method for analyzing the Scatchard plot (Figure 1.8). The experimental curve may be considered to be composed of two straight lines. Their slopes are taken from both end parts of the original curve and they are moved in a parallel manner so that the sum of their ordinate intercepts corresponds to the ordinate intercept of the resulting curve. Lines drawn through the coordinate origin meet the resulting curve at a point  $p$ . Its coordinates are the sums of the coordinates of the respective intersection points of the individual curves, as described for Figure 1.8. For an appropriate evaluation, a computer analysis is strongly recommended (Weder *et al.*, 1974).

Nevertheless, the analysis of such binding curves has only indicative character. On the one hand, there is no essential difference in the resulting curves with two or more binding classes; on the other hand, also other binding mechanisms yield similar curves, such as negative cooperativity and half-of-the-sites reactivity



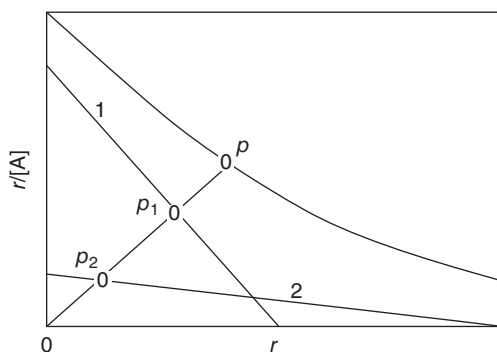


**Figure 1.8** Graphic analysis of a binding curve with two binding classes according to Rosenthal (1967). 1 and 2 are the lines of the separate binding classes. A straight line is drawn from the coordinate origin with the slope  $1/[A]$ , intersecting the individual lines at  $p_1$  and  $p_2$  and the resulting curve at  $p$ . The sum of the coordinates  $[A]_{\text{bound}}$  and  $[A]_{\text{bound}}/[A]$  of the individual intersection points must yield the coordinates of the resulting curve; otherwise, the position of the individual lines must be changed.

(see Section 2.2.2) or isoenzymes. Determination of the number and identity of the subunits of the macromolecule by other methods, such as molecular mass determination, should be performed in parallel.

## References

### Diffusion

- Berg, H.C. (1983) *Random Walks in Biology*, Princeton University Press, Princeton, NJ.
- Berg, O.G. (1985) Orientation constraints in diffusion-limited macromolecular association. *Biophys. J.*, **47**, 1–14.
- McCammon, J.A. and Northrup, S.H. (1981) Gated binding of ligands to protein. *Nature*, **293**, 316–317.
- Noyes, R.M. (1961) Effects of diffusion rates in chemical kinetics. *Prog. React. Kinet.*, **1**, 129–160.

### Binding Equilibria

- Klotz, I.M. (1985) Ligand–receptor interactions: facts and fantasies. *Quart. Rev. Biophys.*, **18**, 227–259.
- Langmuir, I. (1916) The constitution and fundamental properties of solids and liquids. *J. Am. Chem. Soc.*, **38**, 2221–2295.

### Competition

- Thomä, N. and Goody, R.S. (2003) in *Kinetic Analysis of Macromolecules: A Practical Approach* (ed. K.A. Johnson), Oxford University Press, Oxford.

### Graphic Methods

- Huang, C.Y. (1982) Determination of binding stoichiometry by the continuous variation method: the Job plot. *Methods Enzymol.*, **87**, 509–525.

- Job, P. (1928) Recherches sur la Formation de Complexes Minéraux en Solution, et sur leur Stabilité. *Ann. Chim. (Paris)*, **9**, 113–203.
- Klotz, I.M. (1946) The application of the law of mass action to binding by proteins. Interaction with calcium. *Arch. Biochem.*, **9**, 109–117.
- Renny, J.S., Tomasevich, L.L., Tallmagde, E.H., and Collum, D.B. (2013) Method of continuous variations: applications of Job plots to the study of molecular associations in organometallic chemistry. *Angew. Chem. Int. Ed.*, **52**, 11998–12013.
- Rosenthal, H.R. (1967) A graphic method for determination and presentation of binding parameters in a complex system. *Anal. Biochem.*, **20**, 515–532.
- Scatchard, G. (1949) Attractions of proteins for small molecules and ions. *Ann. NY. Acad. Sci.*, **51**, 660–672.
- Stockell, A. (1959) The binding of diphosphopyridine nucleotide by yeast glyceraldehyde-3-phosphate dehydrogenase. *J. Biol. Chem.*, **234**, 1286–1292.
- Weder, H.G., Schildknecht, J., Lutz, L.A., and Kesselring, P. (1974) Determination of binding parameters from Scatchard plots. Theoretical and practical considerations. *Eur. J. Biochem.*, **42**, 475–481.